J Fluoresc (2011) 21:1969–1977
DOI 10.1007/s10895-011-0896-1

ORIGINAL PAPER

Synthesis and Characterization of Triphenylethylene Derivatives with Aggregation-Induced Emission Characteristics

Xiao-Fang Li · Zhen-Guo Chi · Bing-Jia Xu · Hai-Yin Li · Xi-Qi Zhang · Wei Zhou · Yi Zhang · Si-Wei Liu · Jia-Rui Xu

Received: 26 September 2010 / Accepted: 2 May 2011 / Published online: 21 May 2011

Abstract New aggregation-induced emission (AIE) compounds derived from triphenylethylene were synthesized. The thermal, photophysical, electrochemical and aggregation-induced emissive properties were investigated. All the compounds had strong blue light emission capability and good thermal stability. Their maximum fluorescence emission wavelengths were between 443 to 461 nm in solid states, while their glass transition temperatures ranged from 86 to 129 °C. The decomposition temperatures of the synthesized compounds were in the range of 432–534 °C. The synthesized compounds possessed aggregation-induced emission properties, namely exhibited enhanced fluorescence emission in aggregated states. The highest occupied molecular orbital (HOMO) energy levels estimated from the oxidation potentials were between 5.61 and 5.66 eV and the lowest unoccupied molecular orbital/highest occupied molecular orbital (LUMO/HOMO) energy gap values were found to be in the range of 3.18–3.22 eV. The compounds 4-(4-(2,2-bis(4-(naphthalen-1-yl)phenyl)vinyl)phenyl) dibenzothiophene [$(BN)_2Bt$] and 4-(4-(2,2-di(biphenyl-4-yl)vinyl)phenyl) dibenzothiophene [$(BB)_2Bt$] exhibited vibronic fine-structure photoluminescence spectra when the water fraction was less than 70%.

Keywords Triphenylethylene · Blue light emission · Thermal property stability · Synthesis · Aggregation-induced emission

Introduction

Organic luminescent materials with aggregation-induced emission (AIE) properties have attracted considerable attention because of their potential application in electroluminescence devices and chemosensors [1, 2]. Since the first AIE compound 1-methyl-1,2,3,4,5-pentaphenylsilole was reported in 2001 by Tang's group [3], aggregation-caused quenching (ACQ) is no longer the almost insurmountable obstacle in the fabrication of efficient electroluminescent (EL) devices it once was. Since then, some AIE compounds have been developed by various research groups, examples of which include silole, 1,1,2,2-tetraphenylethene (TPE) and 1-cyanotrans-1,2-bis-(4-methylbiphenyl) ethylene (CN-MBE) derivatives [4–11]. However, the AIE materials are still limited in number due to complicated and difficult preparation. Recently, a series of triphenylethylene carbazole and triphenylethylene derivatives with strong light emission, high thermal stability, and AIE characteristics were facilely synthesized via Wittig-Horner and Suzuki reactions in our laboratory [12–21]. The twisted configuration of the three phenyl rings in triphenylethylene, due to the bulky aryl substituents, is considered as one of the possible reasons for the AIE effect.

In this article, we report a new class of triphenylethylene derivatives with strong blue light emission in solid state and AIE characteristics. The derivatives were easily prepared by

Electronic supplementary material The online version of this article (doi:10.1007/s10895-011-0896-1) contains supplementary material, which is available to authorized users.

X.-F. Li · Z.-G. Chi (✉) · B.-J. Xu · H.-Y. Li · X.-Q. Zhang · W. Zhou · Y. Zhang · S.-W. Liu · J.-R. Xu (✉)
PCFM Lab, DSAPM Lab, KLGHEI of Environment and Energy Chemistry, FCM Institute, State Key Laboratory of Optoelectronic Materials and Technologies, School of Chemistry and Chemical Engineering, Sun Yat-Sen University,
Guangzhou 510275, China
e-mail: chizhg@mail.sysu.edu.cn

J.-R. Xu
e-mail: xjr@mail.sysu.edu.cn

a three-step reaction, including the Suzuki and Wittig–Horner reactions. The thermal, photophysical, and AIE properties were preliminarily evaluated.

Experimental

Materials and Methods

Bis(4-bromophenyl)methanone, 4,4′-diphenylbenzophenone, phenylboronic acid, naphthalen-1-ylboronic acid, dibenzothiophene-4-boronic acid, dibenzofuran-4-boronic acid, diethyl 4-bromobenzylphosphonate, tetrakis(triphenylphosphine) palladium(0), tetrabutylammonium bromide (TBAB), potassium *tert*-butyloxide and tetrabutylammonium perchlorate (*n*-Bu_4NClO_4, electrochemical grade) purchased from Alfa Aesar were used as received. All other reagents and solvents were purchased as analytical grade from Guangzhou Dongzheng Company (China) and used without further purification. Anhydrous tetrahydrofuran (THF) was distilled from sodium/benzophenone. Ultrapure water was used in the experiments.

^1H NMR and ^{13}C NMR spectra were measured on a Mercury-Plus 300 spectrometer [$CDCl_3$ as solvent and tetramethylsilane (TMS) as the internal standard]. The Fourier transform infrared (FTIR) spectra were recorded on a Nicolet Nexus 670 spectrometer in the region of 3000–400 cm^{-1}. Mass spectra (MS) were measured on a Thermo DSQ MS spectrometer. Elemental analyses (EA) were performed with an Elementar Vario EL elemental analyzer. Fluorescence spectra were measured on a Shimadzu RF-5301pc spectrometer with a slit width of 1.5 nm for excitation and 3.0 nm for emission. Differential scanning calorimetry (DSC) curves were obtained with a NETZSCH thermal analyzer (DSC 204F1) at heating and cooling rates of 10 °C/min under nitrogen atmosphere. Thermogravimetric analyses (TGA) were performed with a thermal analyzer (Shimadzu, TGA-50H) under nitrogen atmosphere with a heating rate of 20 °C/min. The fluorescence quantum yields (Φ_{FL}) of all the compounds in different solvents and THF/water mixtures were evaluated using 9,10-diphenylanthracene as the reference [22]. Cyclic voltammetry (CV) measurements were carried out on Shanghai Chenhua electrochemical workstations CHI660C in a three-electrode cell with a Pt disk counter electrode, an Ag/AgCl reference electrode, and a glassy carbon working electrode. All CV measurements were performed under an inert argon atmosphere with supporting electrolyte of 0.1 M *n*-Bu_4NClO_4 in dichloromethane at scan rate of 100 mV/s using ferrocene as standard. The lowest unoccupied molecular orbital/highest occupied molecular orbital (LUMO/HOMO) energy gaps ΔEg for the compounds were estimated from the absorption edge of UV–vis absorption spectra.

The water/THF mixtures with different water fractions were prepared by slowly adding ultra-pure water into the THF solution of samples under ultrasound at room temperature. For example, a 70% water fraction mixture was prepared in a volumetric flask by adding 7 mL ultra-pure water into 3 mL THF solution of the sample. The concentrations of all samples were adjusted to 10 μM after adding ultra-pure water.

General Procedure for the Synthesis of Ketone Intermediates $(Ar_1)_2$-one

Bis(4-bromophenyl)methanone (4.6 mmol) and arylboronic acid (11.0 mmol) were dissolved in the mixture of toluene (30 mL), TBAB (0.5 g) and 2 M potassium carbonate aqueous solution (8 mL). The mixture was stirred at room temperature for 0.5 h under argon followed adding Pd$(PPh_3)_4$ (0.01 g) and then heated to 85 °C for 16 h. After that the mixture was poured into water and extracted three times with ethyl acetate. The organic layer was dried over anhydrous sodium sulfate. After removing the solvent under reduced pressure, the residue was chromatographed on a silica gel column with *n*-hexane-CH_2Cl_2 mixed solvent as eluent to give $(Ar_1)_2$-one. Note: in this paper, Ar_1 and Ar_2 represent aryl groups and are identified in Scheme 1.

$(BN)_2$-one White powder, yield 90%. ^1H NMR (300 MHz, $CDCl_3$) δ(ppm) : 8.13-8.01 (d, 4H), 8.00-7.82 (t, 6H), 7.73-7.62 (d, 4H),7.62-7.35 (m, 8H); ^{13}C NMR (75 MHz, $CDCl_3$) δ (ppm): 145.43, 139.36, 136.79, 134.09, 131.55, 130.36, 128.66, 127.25, 126.64, 126.25, 125.90, 125.61; MS (EI), *m/z* : 434 ($[M]^+$, calcd for $C_{33}H_{22}O$, 434); FTIR (KBr) ν(cm^{-1}): 3047, 1654, 1599, 1507, 1393, 1311, 1279, 1180, 929, 779, 690; Anal. calc. for $C_{33}H_{22}O$: C 91.21, H 5.10, O 3.68; Found: C 91.16, H 5.13.

$(BFu)_2$-one White powder, yield 80%. ^1H NMR (300 MHz, $CDCl_3$) δ (ppm): 8.09 (S, 8H), 8.04-7.96 (d, 4H), 7.73-7.60 (dd, 4H), 7.54-7.44 (dd, 4H), 7.43-7.34 (t, 2H); ^{13}C NMR (75 MHz, $CDCl_3$) δ (ppm): 195.93, 156.34, 153.54, 140.75, 136.93, 130.69, 128.86, 127.65, 127.07, 125.41, 124.23, 123.55, 123.18, 120.96, 120.79, 112.11; MS (EI), *m/z*: 514 ($[M]^+$, calcd for $C_{37}H_{22}O_3$, 514); FTIR (KBr) ν (cm^{-1}): 3048, 1652, 1604, 1448, 1393, 1280, 1185, 930, 865, 746, 685; Anal. calc. for $C_{37}H_{22}O_3$: C 86.36, H 4.31, O 9.33; Found: C 86.32, H 4.35.

General Procedure for the Synthesis of Bromide Intermediates $(Ar_1)_2$Br

A solution of compound $(Ar_1)_2$-one (1.84 mmol) and diethyl 4-bromobenzylphosphonate (3.68 mmol) in anhydrous tetrahydrofuran (50 mL) was stirred under an argon

Scheme 1 Synthetic routes to the compounds

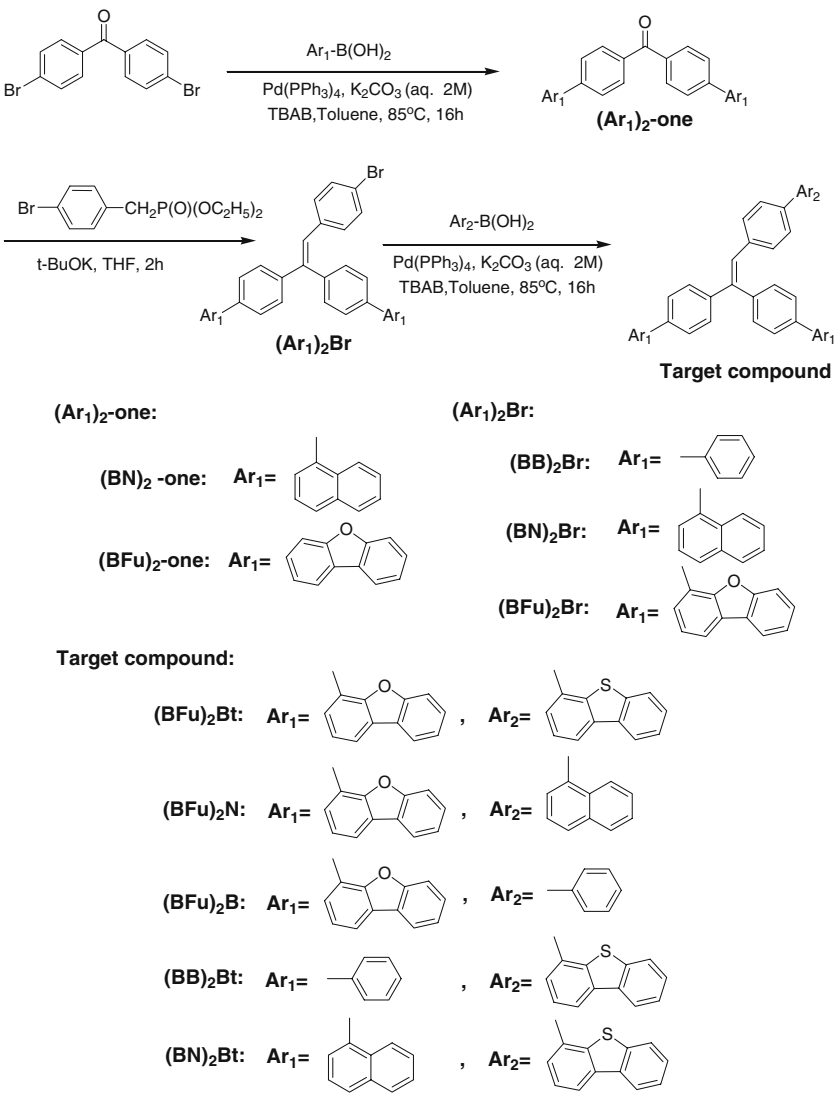

atmosphere at room temperature. Potassium tert-butyloxide (5.54 mmol) was added quickly and the mixture was stirred continuously for 2 h at room temperature. The reaction mixture was precipitated into ethanol, the crude product was collected, and washed with ethanol three times. The crude product was recrystallized from dichloromethane/ethanol (1:20, *v*/*v*) to obtain white powder $(Ar_1)_2Br$.

$(BB)_2Br$ White powder, yield 80%. ^{1}H NMR (300 MHz, $CDCl_3$) δ(ppm): 7.70-7.59 (m, 6H), 7.59-7.55 (d, 2H), 7.51-7.46 (d, 2H), 7.46-7.40 (d, 4H), 7.40-7.34 (m, 2H), 7.32-7.26 (m, 4H), 7.00-6.96 (d, 2H), 6 .95 (s, 1H); ^{13}C NMR (75 MHz, $CDCl_3$) δ (ppm): 142.82, 142.20, 140.76, 140.65, 140.54, 139.01, 136.51, 133.32, 132.05, 131.37, 131.30, 130.98, 129.02, 128.28, 127.58, 127.18, 120.87; MS(EI), *m*/*z*: 486 ([M]$^+$, calcd for $C_{32}H_{23}Br$, 486); FTIR (KBr) ν (cm^{-1}): 3026, 1551, 1517, 1488, 1225, 1075, 1005, 839, 766, 743, 697; Anal. calc. for $C_{32}H_{23}Br$: C 78.85, H 4.76, Br 16.39; Found: C 78.87, H 4.73.

$(BN)_2Br$ White powder, yield 92%. ^{1}H NMR (300 MHz, $CDCl_3$) δ (ppm): 8.04-7.85 (m, 6H), 7.60-7.46 (m, 14H), 7.43-7.38 (d, 2H), 7.38-7.31 (d, 2H), 7.11-7.04 (d, 2H), 7.02 (s, 1H); ^{13}C NMR (75 MHz, $CDCl_3$) δ (ppm): 143.11, 142.03, 140.55, 140.38, 139.98, 139.03, 136.63, 134.07, 132.07, 131.75, 131.40, 130.79, 130.49, 130.31, 128.61, 128.21, 128.04, 127.73, 127.41, 127.23, 127.14, 126.77, 126.38, 126.31, 126.20, 126.05, 125.63, 120.96; MS (EI), *m*/*z*: 586 ([M]$^+$, calcd for $C_{40}H_{27}Br$, 586); FTIR (KBr) ν (cm^{-1}): 3035, 1587, 1507, 1397, 1249, 1070, 1014, 959, 842, 804, 779, 658; Anal. calc. for $C_{40}H_{27}Br$: C 81.77, H 4.63, Br 13.60; Found: C 81.73, H 4.66.

$(BFu)_2Br$ White powder, yield 77%. ^{1}H NMR (300 MHz, $CDCl_3$) δ (ppm) : 8.01-7.88 (m, 8H), 7.70-7.62 (t, 2H), 62–7.54 (t, 4H), 7.50-7.44 (m, 2H), 7.44-7.39 (m, 4H), 7.38-7.32 (m, 2H), 7.31-7.26 (d, 2H), 7.03 (s, 2H), 7.00 (s, 1H); ^{13}C NMR (75 MHz, $CDCl_3$) δ (ppm): 155.89, 153.13, 142.57, 142.23, 139.04, 136.11, 135.64, 135.55, 131.02,

130.46, 128.86, 128.44, 127.79, 127.05, 126.47, 125.14, 125.01, 124.87, 124.79, 123.96, 123.04, 122.60, 120.47, 119.62, 119.56, 111.70; MS(EI), *m/z*: 666 ($[M]^+$, calcd for $C_{44}H_{27}BrO_2$, 666); FTIR (KBr) ν(cm^{-1}): 3032, 2359, 1587, 1513, 1481, 1450, 1393, 1260, 1190, 1067, 1011, 874, 842, 795, 750; Anal. calc. for $C_{44}H_{27}BrO_2$: C 79.16, H 4.08, Br 11.97, O 4.79; Found: C 79.13, H 4.12.

General Procedure for the Synthesis of the Target Compounds

To a solution of $(Ar_1)_2Br$ (0.75 mmol), corresponding boric acid (0.90 mmol) and TBAB (0.5 g) in toluene (35 mL), 2 M aqueous K_2CO_3 solution (1.5 mL) was added and the mixture was stirred for 30 min under an argon atmosphere. Then, the $Pd(PPh_3)_4$ catalyst (0.01 g) was added all at once to the mixture. The reaction mixture was stirred at 85 °C for 16 h. After cooling, the product was extracted with dichloromethane/water. The organic layers were collected and dried under anhydrous sodium sulfate. The concentrated product was purified by silica gel column chromatography (dichloromethane-*n*-hexane mixed solvent as eluent) to obtain target products.

(BFu)$_2$B White powder, yield 30%. ^{1}H NMR (300 MHz, $CDCl_3$) δ (ppm): 8.04-7.98 (t, 4H), 7.98-7.93 (m, 4H), 74–7.71 (d, 1H), 7.67-7.65 (d, 1H), 7.64-7.56 (m, 6H), 7.54-7.39 (m, 11H), 7.38-7.34 (d, 2H), 7.33-7.27 (t, 2H), 7.18 (s, 1H); ^{13}C NMR (75 MHz, $CDCl_3$) δ (ppm): 155.89, 153.13, 142.54, 141.77, 140.31, 139.54, 139.20, 136.19, 135.40, 135.34, 130.55, 129.87, 128.82, 128.47, 128.40, 127.95, 127.76, 127.00, 126.61, 126.47, 125.21, 125.13, 124.84, 124.76, 123.96, 123.01, 122.55, 120.44, 119.47, 111.66; MS (EI), *m/z*: 664 ($[M]^+$, calcd for $C_{50}H_{32}O_2$, 664); FTIR(KBr) ν (cm^{-1}): 3029, 2370, 1590, 1517, 1483, 1448, 1394, 1264, 1190, 1008, 875, 840, 751, 696; Anal. calc. for $C_{50}H_{32}O_2$: C 90.33, H 4.85, O 4.81; Found: C 90.30, H 4.88.

(BFu)$_2$N White powder, yield 37%. ^{1}H NMR (300 MHz, $CDCl_3$) δ (ppm) : 8.05-7.96 (t, 4H), 7.96-7.92 (m, 4H), 7.88-7.83 (d, 1H), 7.83-7.78 (d, 1H), 7.72-7.68 (d, 1H), 7.66-7.63 (d, 2H), 7.62-7.58 (d, 3H), 7.56-7.51 (d, 2H), 7.51-7.34 (m, 11H), 7.34-7.28 (t, 4H),7.22 (s, 1H); ^{13}C NMR (75 MHz, $CDCl_3$) δ (ppm): 155.93, 153.17, 142.61, 141.88, 139.63, 139.10, 136.14, 135.46, 133.60, 131.25, 130.58, 129.67, 129.36, 128.89, 128.45, 128.06, 127.80, 127.38, 127.02, 126.65, 126.51, 125.77, 125.51, 125.24, 125.15, 124.86, 123.99, 123.04, 122.58, 120.47, 119.53, 111.69; MS(EI), *m/z*: 714 ($[M]^+$, calcd for $C_{54}H_{34}O_2$, 714); FTIR (KBr) ν (cm^{-1}): 3059, 1583, 1557, 1539, 1519, 1450, 1393, 1260, 1190, 869, 841, 794, 774, 748; Anal. calc. for $C_{54}H_{34}O_2$: C 90.73, H 4.79, O 4.48; Found: C 90.76, H 4.77.

(BFu)$_2$Bt Light green powder, yield 30%. ^{1}H NMR (300 MHz, $CDCl_3$) δ (ppm): 8.16-8.07 (m, 2H), 8.05-7.89 (m, 8H), 7.80-7.75 (dd, 1H), 7.73-7.69 (d, 1H), 7.65-7.62 (d, 2H), 7.61-7.57 (t, 4H), 7.55-7.39 (m, 10H), 7.38-7.29 (m, 4H),7.23 (s, 1H),7.20 (s, 1H); ^{13}C NMR (75 MHz, $CDCl_3$) δ (ppm): 156.34, 153.58, 142.94, 142.64, 139.88, 139.73, 139.17, 138.56, 137.32, 136.77, 136.44, 135.93, 131.01, 130.28, 129.31, 128.86, 128.25, 128.15, 127.44, 126.94, 125.64, 125.27, 124.53, 124.40, 123.45, 122.99, 122.79, 121.88, 120.60, 119.95, 112.13; MS(EI), *m/z*: 770 ($[M]^+$, calcd for $C_{56}H_{34}O_2S$, 770); FTIR (KBr) ν (cm^{-1}): 3059, 1584, 1517, 1451, 1394, 1257, 1190, 1013, 874, 842, 798, 750; Anal. calc. for $C_{56}H_{34}O_2S$: C 87.24, H 4.45, O 4.15, S 4.16; Found: C 87.21, H 4.46, S 4.18.

(BN)$_2$Bt White powder, yield 50%. ^{1}H NMR (300 MHz, $CDCl_3$) δ (ppm): 8.18-8.09 (m, 2H), 8.06-7.97 (t, 2H), 7.93-7.83 (dd, 4H), 7.80-7.75 (m, 1H), 7.64-7.40 (m, 22H), 7.33-7.27(d, 2H), 7.24-7.22 (d, 1H); ^{13}C NMR (75 MHz, $CDCl_3$) δ (ppm): 142.80, 142.27, 141.94, 140.42, 140.29, 140.14, 140.07, 139.76, 139.43, 139.20, 138.63, 137.43, 136.81, 136.48, 135.98, 134.25, 134.07, 131.81, 130.78, 130.61, 130.29, 128.54, 128.24, 128.11, 127.95, 127.74, 127.21, 127.13, 126.98, 126.38, 126.27, 126.15, 126.02, 125.62, 125.30, 124.57, 122.80, 121.92, 120.65, 109.98; MS(EI), *m/z*: 690 ($[M]^+$, calcd for $C_{52}H_{34}S$, 690); FTIR (KBr) ν (cm^{-1}): 3054, 1587, 1507, 1439, 1390, 1241, 1187, 1107, 1020, 960, 845, 797, 748; Anal. calc. for $C_{52}H_{34}S$: C 90.40, H 4.96, S 4.64; Found: C 90.38, H 4.98, S 4.62.

(BB)$_2$Bt White powder, yield 50%. ^{1}H NMR (300 MHz, $CDCl_3$) δ (ppm): 8.16-8.06 (m, 2H), 7.82-7.75 (t, 1H), 7.69-7.63 (d, 3H), 7.63-7.56 (t, 4H), 7.56-7.51 (d,3H), 7.50-7.37 (m, 11H), 7.37-7.28 (t, 3H), 7.26-7.22 (d, 2H), 7.10 (s, 1H); ^{13}C NMR (75 MHz, $CDCl_3$) δ (ppm): 142.51, 140.83, 140.64, 140.45, 139.72, 139.44, 139.11, 138.54, 137.29, 136.74, 136.44, 135.93, 131.10, 130.20, 129.02, 128.33, 128.10, 128.00, 127.62, 127.22, 126.97, 125.28, 124.56, 122.79, 121.91, 120.62; MS(EI), *m/z*: 590 ($[M]^+$, calcd for $C_{44}H_{30}S$, 590); FTIR (KBr) ν (cm^{-1}): 3026, 2353, 1602, 1481, 1441, 1380, 1249, 1107, 1003, 897, 840, 745, 695; Anal. calc. for $C_{44}H_{30}S$: C 89.45, H 5.12, S 5.43; Found: C 89.41, H 5.15, S 5.40.

Results and Discussion

Synthesis

Our strategy for the synthesis of the new class of triphenylethylene derivatives is outlined in Scheme 1. The target compounds were synthesized by the palladium-

catalyzed Suzuki coupling reactions of aryl bromide intermediates **[$(Ar_1)_2Br$]** with arylboronic acids in moderate yields (30–50%). The **$(Ar_1)_2Br$** were synthesized through simple Wittig-Horner reaction of the ylide reagent diethyl 4-bromobenzylphosphonate with ketone intermediates [**$(Ar_1)_2$-one**] in high yields (77–92%). The **$(Ar_1)_2$-one** were also prepared by the Suzuki coupling reactions of bis(4-bromophenyl)methanone (4.6 mmol) and the corresponding arylboronic acids with high yields (66–90%). The products were purified by recrystallization or column chromatography on silica gel using dichloromethane-*n*-hexane as eluent. Their molecular structures were confirmed with ^{1}H-NMR, ^{13}C-NMR, MS and FTIR and EA.

For the comparison purposes, the five target compounds were divided into two classes. In one class, the Ar_1 was dibenzofuran ring and the Ar_2 were phenyl, naphthalene and dibenzothiophene rings with increasing size of substituent [Class I: $(BFu)_2B$, $(BFu)_2N$, and $(BFu)_2Bt$]. In the other class, the Ar_2 was the same (dibenzothiophene ring) and the Ar_1 were different. The Ar_1 were changed according to the increasing size of substituent: phenyl, naphthalene and dibenzofuran rings [Class II: $(BB)_2Bt$, $(BN)_2Bt$ and $(BFu)_2Bt$].

Thermal Properties

The thermal stability of organic materials is crucial for EL device stability and lifetime. The thermal instability or low glass transition temperature (T_g) of the amorphous organic materials may result in the degradation of EL device due to morphological changes during the device operation. Hence, a relatively high T_g is essential for emissive materials used in optoelectronic applications.

Thermal properties of the compounds were investigated by differential scanning calorimetry (DSC) and thermal gravimetric analysis (TGA). Their DSC and TGA curves are shown in Figs. 1 and 2, respectively, and the data are summarized in Table 1. The T_g values of $(BFu)_2B$, $(BFu)_2N$, $(BFu)_2Bt$, $(BN)_2Bt$ and $(BB)_2Bt$ are 110, 117, 129, 108 and 86 °C, which are higher than those of the two typical AIE compounds reported, 1-methyl-1,2,3,4,5-pentaphenylsilole (MPPS, 54 °C) and 1,1,2,3,4,5-hexaphenyl silole (HPS, 65 °C) [23]. As expected, T_g values of either Class I compounds or Class II compounds increased with the increasing size of substituent. For example, in Class II, the T_g of $(BFu)_2Bt$ with the largest substituent dibenzofuran ring is 43 °C higher than that of $(BB)_2Bt$ with the smallest substituent phenyl ring. Thus the incorporation of a bulky substituent in molecular structure can greatly improve glassy-state durability.

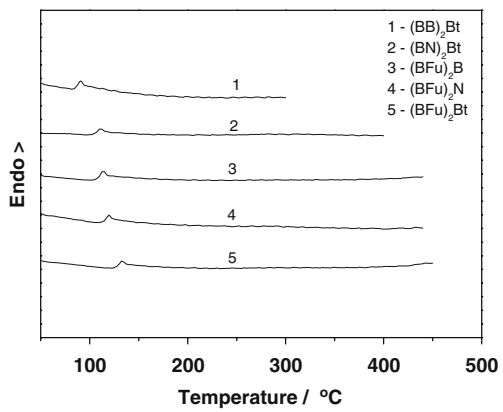

Fig. 1 DSC curves for the compounds at a scan rate of 10 °C/min (second heating scan)

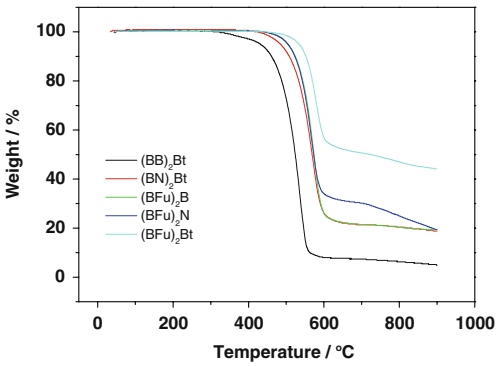

Fig. 2 TGA curves of the compounds

From Fig. 1, it can be seen that the DSC curve of each compound in second heating run exhibits only a glass transition. This indicates that the compounds have an extremely low tendency toward crystallization from their melts. No melting peak could be detected in the second heating runs, which was ascribed to the non-planar and propeller-like chemical structure of substituent triphenylethylene making it difficult for them to assume a dense packing structure.

The decomposition temperatures with 5% weight loss under nitrogen atmosphere (T_d) of $(BFu)_2B$, $(BFu)_2N$, $(BFu)_2Bt$, $(BN)_2Bt$ and $(BB)_2Bt$ are 505, 505, 534, 484 and 432 °C, respectively. The T_d values, as expected, also increase with the increasing size of the substituent, similar to the change of T_g.

Table 1 The thermal properties of the compounds

	T_g/°C	T_d/°C(weight loss 5%)
$(BFu)_2B$	110	505
$(BFu)_2N$	117	505
$(BFu)_2Bt$	129	534
$(BN)_2Bt$	108	484
$(BB)_2Bt$	86	432

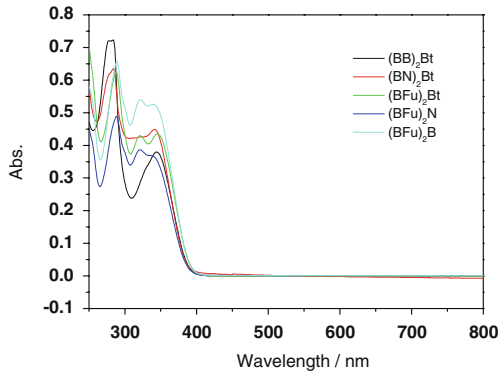

Fig. 3 UV absorption spectra of the compounds in THF (10 μM)

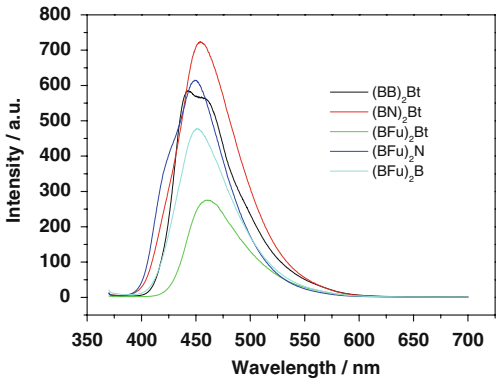

Fig. 5 Photoluminescence emission spectra of the compounds in solid powders upon excitation at 365 nm

Photophysical and Electrochemical Properties

As shown in Fig. 3, the Class I compounds containing dibenzofuran rings, $(BFu)_2B$, $(BFu)_2N$ and $(BFu)_2Bt$, can exhibit three absorption bands centered at 289, 322 and ~340 nm, respectively. The fact that the former two bands remain unchanged indicates that the two absorption bands correspond to the absorption of dibenzofuran rings. The absorption band at ~340 nm is ascribed to the π-π* transition of the whole conjugated π-electron system. There are two main absorption bands in the compounds $(BN)_2Bt$ and $(BB)_2Bt$: one located at about 284 nm could be assigned to the absorption of the dibenzothiophene ring, and the other located at about 340 nm is also attributed to the π-π* transition of the whole conjugated π-electron system. It is interesting to note that the two compounds $(BFu)_2N$ in Class I and $(BN)_2Bt$ in Class II containing naphthalene ring have shorter absorption of the π-π* transition of the whole conjugated π-electron system. This indicates that, although naphthalene ring [in $(BFu)_2N$ and $(BN)_2Bt$] has longer conjugation than phenyl ring [in $(BFu)_2B$ and $(BB)_2Bt$], the naphthalene ring substituents cannot improve the molecular π- conjugation extents, however, they shorten π-conjugation due to more twisted conformation caused by the effect of steric hindrance of naphthalene ring.

Surprisingly, the photoluminescence (PL) spectra (Fig. 4) of the three compounds containing dibenzofuran rings are very similar, and the maximum emission wavelengths (λ_{max}^{em}) are found at about 464 nm. This strongly suggests that the Ar_2 substituents do not affect the electron transition energy from excited state to the ground state. However, the compounds $(BN)_2Bt$ and $(BB)_2Bt$ exhibit vibronic fine-structure PL spectra and significant blue-shift in the emission spectra. At the same concentration (10 μM), $(BN)_2Bt$ shows the strongest PL intensity among the compounds, and $(BB)_2Bt$ is the weakest one.

The PL spectra of the compounds in solid powder states are shown in Fig. 5. The λ_{max}^{em} values of $(BFu)_2B$, $(BFu)_2N$, $(BFu)_2Bt$, $(BN)_2Bt$ and $(BB)_2Bt$ are 452, 450, 461, 454 and 443 nm, respectively. In Class I, comparing the λ_{max}^{em} values of the compounds, it can found that the Ar_2 substituents affect the λ_{max}^{em} values. Compared with $(BFu)_2Bt$, the λ_{max}^{em} of $(BFu)_2B$ and $(BFu)_2N$ with smaller substituents exhibit significant blue-shift by 9 and 11 nm, respectively. However,

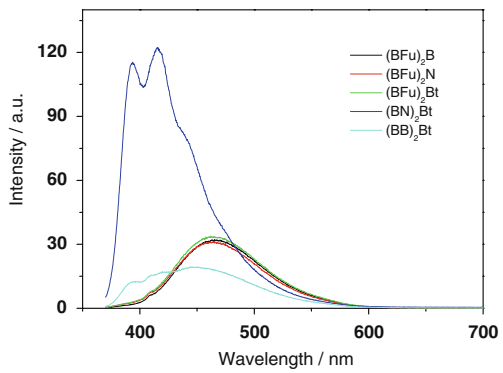

Fig. 4 Photoluminescence emission spectra of the compounds in THF (10 μM) upon excitation at 365 nm

Table 2 Optical properties of the compounds

	λ^{abs}/nm	λ^{em}/nm		Φ_{FL}/%
	[a]	[b]	[c]	[d]
$(BFu)_2B$	289,322,341	465	452	1.0
$(BFu)_2N$	289,322,338	464	450	1.5
$(BFu)_2Bt$	289,322,346	464	461	1.1
$(BN)_2Bt$	284,342	415	454	3.8
$(BB)_2Bt$	284,345	448	443	0.9

[a] In THF

[b] In THF

[c] Solid powder

[d] Fluorescence quantum yields measured in THF solution

Table 3 Energy levels of the compounds

	HOMO/eV	LUMO/eV	ΔEg/eV
$(BFu)_2B$	5.61	2.41	3.20
$(BFu)_2N$	5.63	2.41	3.22
$(BFu)_2Bt$	5.64	2.46	3.18
$(BN)_2Bt$	5.66	2.44	3.22
$(BB)_2Bt$	5.64	2.44	3.20

in Class II compared with $(BFu)_2Bt$, the $(BN)_2Bt$ shows a 7 nm blue-shift and $(BB)_2Bt$ shows a 18 nm blue-shift.

Comparing the λ_{max}^{em} values of the compounds in THF solutions and in the solid states, the compounds $(BFu)_2B$ and $(BFu)_2N$ exhibit significant blue-shift by 13 and 14 nm, respectively. However, the $(BN)_2Bt$ shows a 39 nm red-shift and $(BB)_2Bt$ shows a 5 nm blue-shift. This indicates that different substituting groups and their sites affect the intermolecular interaction and molecular packing which strongly affect their solid emission.

Similar to other reported AIE materials, the synthesized compounds exhibit weak emission when dissolved as dispersed molecules in good solvents, as can be seen from low PL intensity and low fluorescence quantum yield

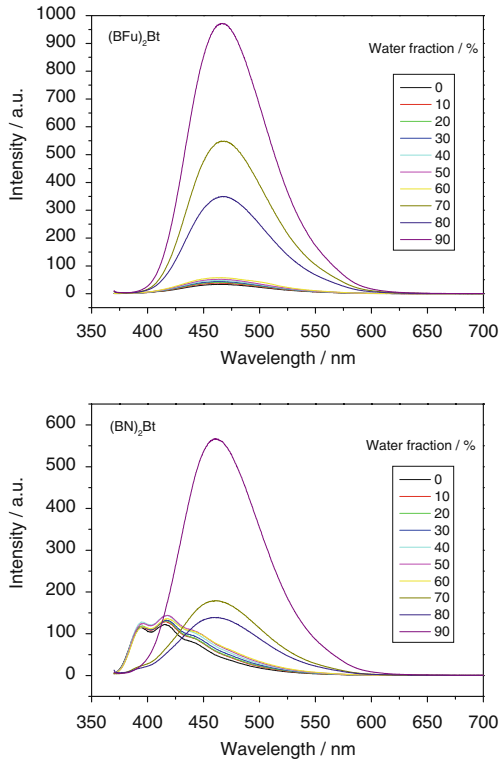

Fig. 6 Photoluminescence spectra of $(BFu)_2Bt$ and $(BN)_2Bt$ in water/THF mixtures (10 μM) with different volume fractions of water upon excitation at 365 nm

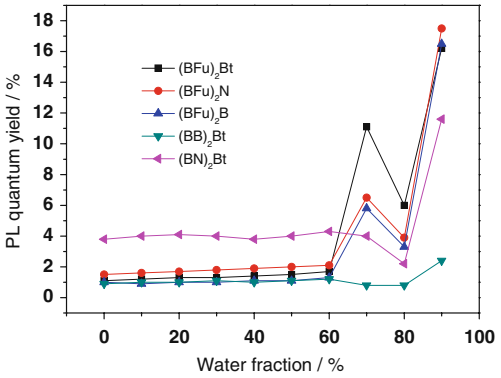

Fig. 7 Photoluminescence quantum yields of the compounds in water/THF mixtures with water fraction (10 μM)

(Φ_{FL}). For example, the 10 μM THF solutions of the compounds show low Φ_{FL} values less than 3.8% (Table 2).

The highest occupied molecular orbital (HOMO), lowest unoccupied molecular orbital (LUMO) and energy band gaps (ΔE_g) are three important parameters for electroluminescent materials. By cyclic voltammetry (CV) analyses and UV absorption spectra, the HOMO energy levels and ΔE_g were obtained using the onset oxidation potential in the CV curve (Fig. S1) and from the onset wavelength of their UV absorption spectra, respectively. Then, the LUMO energy levels were obtained from the HOMO energy and energy band gap (ΔE_g=HOMO−LUMO). Table 3 shows that the energy levels of the compounds are very close to each other. The HOMO levels of these compounds are between 5.61 and 5.66 eV. This suggests that the synthesized compounds have potential as a hole transporting materials. The ΔE_g values of the compounds were found to be in the range of 3.18–3.22 eV. The LUMO values ranged from 2.41 to 2.46 eV.

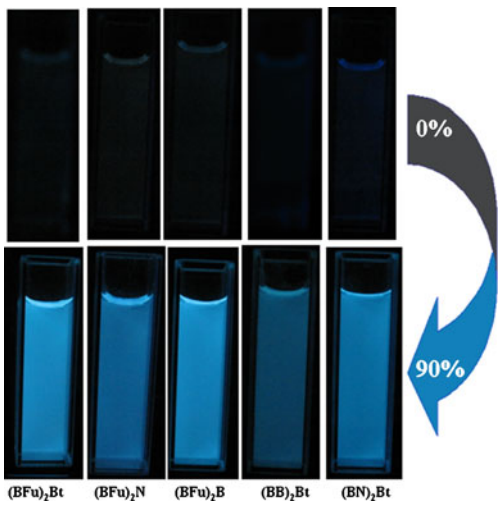

Fig. 8 Emission images of the compounds in pure THF (10 μM) and in water/THF mixture with 90% water fraction under UV light (365 nm) illumination

AIE Properties

To determine whether or not these compounds are AIE active, the UV absorption and PL emission behaviors of their diluted mixtures were studied in a mixture of water/THF with different water fractions. Since the compounds were insoluble in water, increasing the water fraction in the mixed solvent could thus change their existing forms from a solution or well-dispersed state in pure THF to aggregated particles in the mixtures with high water content, which results in changes in the UV and PL spectra.

The PL spectra of 10 μM of $(BFu)_2Bt$ and $(BN)_2Bt$ in water/THF mixtures with different water contents are shown in Fig. 6 as examples (the others are shown in Fig. S2). For $(BFu)_2Bt$ in pure THF and in the mixtures with water fraction <60% exhibited very weak PL intensity. However, the fluorescent intensity was significantly enhanced when the water fraction exceeded 60%, and when the water fraction was up from 70% to 80%, the PL intensity exhibited a decrease. Similar effects were observed for the compounds $(BFu)_2N$ and $(BFu)_2B$ (Fig. 7). This phenomenon was often observed in some compounds with AIE properties, but the reasons remain unclear. Although the PL intensities of the Class I compounds changed with the increase of water fraction, the position of peaks showed almost no change.

However, the compounds $(BN)_2Bt$ and $(BB)_2Bt$ exhibited vibronic fine-structure PL spectra when the water fraction was less than 70%. When the water fraction was up to 70%, the PL spectrum had a significant change with the disappearance of the fine-structure, and the maximum emission wavelength exhibited a significant red-shift. The difference was also reflected in PL quantum yields (Fig. 7).

The emission images of the compounds in pure THF and in water/THF mixture with 90% water fraction under UV light (365 nm) illumination at room temperature are shown in Fig. 8. Clearly, THF solutions of the compounds showed very weak fluorescence. However, the compounds in high water fractions of water/THF mixtures exhibited very strong fluorescence confirming that the emission enhancements were induced by the aggregation of the molecules.

Conclusions

We have developed a new class of AIE compounds, composed of triphenylethylene derivatives. The compounds exhibit a strongly enhanced emission in the aggregated state. The derivatives are all blue light emitters, and their maximum fluorescence emission wavelengths are 443–461 nm in solid states. The glass transition temperatures range is from 86 to 129 °C, and the decomposition temperatures (5% weight loss) are in the range of 432–534 °C, both of which are higher than those silole derivatives ever reported in the literature. The HOMO levels of these compounds are between 5.61 and 5.66 eV and the ΔE_g values were found to be in the range of 3.18–3.22 eV. The compounds $(BN)_2Bt$ and $(BB)_2Bt$ exhibited vibronic fine-structure PL spectra when the water fraction was less than 70%.

Acknowledgments The authors gratefully acknowledge the financial support from the National Natural Science Foundation of China (Grant numbers: 50773096 and 51073177), the Start-up Fund for Recruiting Professionals from "985 Project" of SYSU, the Science and Technology Planning Project of Guangdong Province, China (Grant numbers: 2007A010500001-2, 2008B090500196), Construction Project for University-Industry cooperation platform for Flat Panel Display from the Commission of Economy and Informatization of Guangdong Province (Grant numbers: 20081203), the Fundamental Research Funds for the Central Universities, the Opening Fund of Laboratory Sun Yat-sen University (KF201026), and the Fund for Innovative Chemical Experiment and Research of School of Chemistry and Chemical Engineering.

References

1. Hong YN, Lam JWY, Tang BZ (2009) Aggregation-induced emission: phenomenon, mechanism and applications. Chem Commun 29:4332–4353
2. Zhao YS, Fu HB, Peng AD, Ma Y, Xiao DB, Yao JN (2008) Low-dimensional nanomaterials based on small organic molecules: preparation and optoelectronic properties. Adv Mater 20:2859–2876
3. Luo JD, Xie ZL, Lam JWY, Cheng L, Chen HY, Qiu CF, Kwok HS, Zhan XW, Liu YQ, Zhu DB, Tang BZ (2001) Aggregation-induced emission of 1-methyl-1,2,3,4,5- pentaphenylsilole. Chem Commun 1740–1741
4. An BK, Lee DS, Lee JS, Park YS, Song HS, Park SY (2004) Strongly fluorescent organogel system comprising fibrillar self-Assembly of a trifluoromethyl-based cyanostilbene derivative. J Am Chem Soc 126:10232–10233
5. Chen JW, Xu B, Ouyang XY, Tang BZ, Cao Y (2004) Aggregation-induced emission of *cis*, *cis*-1,2,3,4-tetraphenylbutadiene from restricted intramolecular rotation. J Phys Chem A 108:7522–7526
6. Chen JW, Law CCW, Lam JWY, Dong YP, Lo SMF, Williams ID, Zhu DB, Tang BZ (2003) Synthesis, light emission, nanoaggregation, and restricted intramolecular rotation of 1,1-substituted 2,3,4,5-tetraphenylsiloles. Chem Mater 15:1535–1546
7. Ren Y, Lam JWY, Dong Y, Tang BZ, Wong KS (2005) Enhanced emission efficiency and excited state lifetime due to restricted intramolecular motion in silole aggregates. J Phys Chem B 109:1135–1140
8. Tong H, Dong YQ, Häußler M, Lam JWY, Sung HHY, Williams ID, Sun JZ, Tang BZ (2006) Tunable aggregation-induced emission of diphenyldibenzofulvenes. Chem Commun 10:1133–1135
9. Wang F, Han MY, Mya KY, Wang Y, Lai YH (2005) Aggregation-driven growth of size-tunable organic nanoparticles using electronically altered conjugated polymers. J Am Chem Soc 127:10350–10355
10. Itami K, Ohashi Y, Yoshida JI (2005) Triarylethene-based extended π-systems: programmable synthesis and photophysical properties. J Org Chem 70:2778–2792

11. Bhongale CJ, Chang CW, Lee CS, Diau EWG, Hsu CS (2005) Relaxation dynamics and structural characterization of organic nanoparticles with enhanced emission. J Phys Chem B 109:13472–13482
12. Yang ZY, Chi ZG, Yu T, Zhang XQ, Chen MN, Xu BJ, Liu SW, Zhang Y, Xu JR (2009) Triphenylethylene carbazole derivatives as a new class of AIE materials with strong blue light emission and high glass transition temperature. J Mater Chem 19:5541–5546
13. Xu BJ, Chi ZG, Yang ZY, Chen JB, Deng SZ, Li HY, Li XF, Zhang Y, Xu NS, Xu JR (2010) Facile synthesis of a new class of aggregation-induced emission materials derived from triphenylethylene. J Mater Chem 20:4135–4141
14. Li HY, Chi ZG, Xu BJ, Zhang XQ, Yang ZY, Li XF, Liu SW, Zhang Y, Xu JR (2010) New aggregation-induced emission enhancement materials combined triarylamine and dicarbazolyl triphenylethylene moieties. J Mater Chem 20:6103–6110
15. Yang ZY, Chi ZG, Xu BJ, Li HY, Zhang XQ, Li XF, Liu SW, Zhang Y, Xu JR (2010) High-T_g carbazole derivatives as a new class of aggregation-induced emission enhancement materials. J Mater Chem 20:7352–7359
16. Zhang XQ, Chi ZG, Xu BJ, Li HY, Zhou W, Li XF, Zhang Y, Liu SW, Xu JR (2011) Comparison of responsive behaviors of two cinnamic acid derivatives containing carbazolyl triphenylethylene. J Fluoresc 21:133–140
17. Xu BJ, Chi ZG, Li XF, Li HY, Zhou W, Zhang XQ, Wang CC, Zhang Y, Liu SW, Xu JR (2011) Synthesis and properties of diphenylcarbazole triphenylethylene derivatives with aggregation-induced emission, blue light emission and high thermal stability. J Fluoresc 21:433–441
18. Li HY, Chi ZG, Xu BJ, Zhang XQ, Li XF, Liu SW, Zhang Y, Xu JR (2011) Aggregation-induced emission enhancement compounds containing triphenylamine-anthrylenevinylene and tetraphenylethene moieties. J Mater Chem 21:3760–3767
19. Zhang XQ, Chi ZG, Li HY, Xu BJ, Li XF, Liu SW, Zhang Y, Xu JR (2011) Synthesis and properties of novel aggregation-induced emission compounds with combined tetraphenylethylene and dicarbazolyl triphenylethylene moieties. J Mater Chem 21:1788–1796
20. Zhang XQ, Chi ZG, Xu BJ, Li HY, Yang ZY, Li XF, Liu SW, Zhang Y, Xu JR (2011) Synthesis of blue light emitting bis (triphenylethylene) derivatives: a case of aggregation-induced emission enhancement. Dyes Pigm 89:56–62
21. Zhang XQ, Yang ZY, Chi ZG, Chen MN, Xu BJ, Wang CC, Liu SW, Zhang Y, Xu JR (2010) A multi-sensing fluorescent compound derived from cyanoacrylic acid. J Mater Chem 20:292–298
22. Morris JV, Mahaney MA, Huber JR (1976) Fluorescence quantum yield determinations: 9,10-Diphenylanthracene as a reference standard in different solvents. J Phys Chem 80:969–974
23. Ning ZJ, Chen Z, Zhang Q, Yan YL, Qian SX, Cao Y, Tian H (2007) Aggregation-induced emission (AIE)-active starburst triarylamine fluorophores as potential non-doped red emitters for organic light-emitting diodes and Cl_2 gas chemodosimeter. Adv Funct Mater 17:3799–3807